Original Paper

Studies on Conductance Switching in Iron Oxides

*Masaaki Miyamoto**

Synopsis: Memory switching in electric conduction was found in polycrystalline ferric oxides treated with an electric breakdown. Current-voltage characteristic was symmetric with the polarity of applied voltage, and the switching was observed from 77 to 500 k. A series of experiments demonstrate that space-charge-limited current flows after filling of traps with injected carriers. The sample which shows switching has a filamentary conductive path of magnetite. But the phase of magnetite is covered with a very thin layer of reoxidized hematite. The memory switching occures in magnetite-hematite-magnetite sandwitch structure. Under the condition of current limited, I–V characteristic showed Lampert's triangle. By using the triangle, carrier density n, trap density N_t and electron mobility μ_n were calculated. The threshold voltage of switching changed systematically with the number of cyclic switching. The change of threshold voltage is explainable with the relaxation process such as charge trapping and release. Double-pulse measurement suggested the mechanism of single carrier injection process. Under the condition of large current, threshold voltages begin to change with the switching cycles in the conditions of various surrounding gas atmospheres. The mechanism of this change consists of the structural change of the surface (oxidation or reduction) in magnetite-hematited-magnetite sandwitch structure as the result of Joule heating by the flowing current after every switching. The change of threshold voltage under the various condition of ambient gas is also reported.

1. Introduction

Current-controlled negative resistance (CCNR) has been observed in a variety of oxides such as Nb_2O_5[1,2], NiO[3,4], Cu–doped Fe_2O_3[5], MoO[6], Oxide films of Nb, Ta and Ti[7], TiO_2[8], Cu_2O[9,10], Si–doped YlG[11], SiO_2[12], Cd boracite[13], and SnO_2–VO_x–PdO[14]. Electronic mechanisms such as injection of carriers[1,6,7,11] or others[2,4], and thermal ones[3,9,12] are proposed for the explanation of CCNR. In these oxides, memory switching effects have also been reported[3,9,10,11]. Memory switching effects have been considered to require some structural changes[15]. Electronic effects such as injection of carriers[6], or delocalization of charge carriers[4] and thermodynamic effects such as phase transitions[17,18] or precipitation of metallic phases[9,19] have been proposed as causes of structural changes. The negative resistance in copper-doped Fe_2O_3 ceramic could be ascribed to the difference in oxygen content in the phase[5]. The possibility of magnetite-filament formation has been suggested in Si-doped YlG memory switching[11]. A basic problem of memory switching concerns the origin of the high-conductive state which is attainable after the removal of the source voltage. Negative resistance and memory switching in sintered ferric oxides have reen reported[20,21]. The formation of magnetite filament has been confirmed through the low-temperature measurement of I–V characteristic[22]. In this paper the causes of the change of memory state were clarified by the measurements of I–V characteristics under the various conditions. It was found that SCLC (Space-Charge-Limited-Current) and TFL (Trap-Filled-Limit) theories were useful for explaining the mechanisms of electronic switching in ferric oxide as reported in other materials[13,16,23].

*Assistant Professor, Electrical Engineering Division

2. Sample preparation and measurement

Ferric oxide powder (99.9%: pure sample) and mixed powder with 0–20 mol% oxides (such as ZnO, TiO_2, CuO, NiO: mixed sample) were compacted into discs of 10 mm diameter and 0.3～0.5 mm thick at 1 ton/cm^2 and sintered at 1150–1300 °C in air for two hours. Silver paint (Dupong #6216) was used as electrode material. In order to reduce the sample resistance, breakdown voltage was applied between upper and lower sides electrodes or between two electrodes on one side of the disc using the constant current supplies under the condition of current limited (1～100 mA). This process is called "forming"[20]. Iron films evapolated on the Pt electrode on alumina substrate were oxidized gradualy to magnetite in alkali solution, and oxidized into hematite during one hour heating at 600 °C in air.

Resulting hematite films are 500～1000 nm thick and show memory switching as same as sintered hematite ceramics[24]. This thin films of hematite sandwitched with silver paint and Pt electrode are measured as models of sandwitched structure for the conductive path. (: thin film sample) I–V characteristics were measured with PA DC Voltage source (YHP 4140B) and DC constant current supply. These were connected to micro computer system (NEC PC8801) with GP–IB cable and measured data were stored and treated systematically. Ordinarilly measurement of I–V characteristic in low temperature region were done in vacuum case which was set in the criostat and was connected to the voltage source with triaxial cable and BNC connector. Current limiting voltage source, DC double pulse generator, oscilloscope and X–Y recorder were used for the measurements of continuous cycles of I–V curves and characteristics of the switching phenomena such as change of threshold voltage (V_{th}) or switching delay time or switching time.

3. Results

3.1 Forming process

Electrical breakdown occurred in several seconds after the voltage application. A thin conductive path was formed between the electrodes[20]. The thickness of the path had a tendency to increase with increasing flowing current during the electric breakdown. (In this treatment, constant current-supply was used and current was limited to 100 mA.) Ordinarily, this treatment was done at room temperature in air. A thin conductive path (50～100 μm in diameter) was produced. Apparent resistance of the sample decreased 3–4 orders of magnitude owing to the formation of the conductive path. After the removal of applied voltage, apparent resistance returned to the initial value (10^8–10^{10} ohm), and the sample showed memory switching. Stable switching was observed after flowing an appropriate current. No forming was needed for thin films of hematite to show memory switching[24].

3.2 Threshold voltage of switching

AC I–V characteristic of the formed sample (typical in mixed samples) is shown in Fig. 1.

Initially the sample had a resistance of more than 10^8 ohm. When the increasng voltage applied to the sample, switching from off to on–state occurred at a threshold voltage V_{th}. The sample retained the on-state if the maximum current I_m was sufficient, but the reduction of I_m resulted in the hysteresis effect. In a large current region, orange-red light emission was observed in the conductive path as reported by Lo[5]. Threshold voltage V_{th} in some of the mixed samples changed in accordance with the change of ambient gas condition as shown in

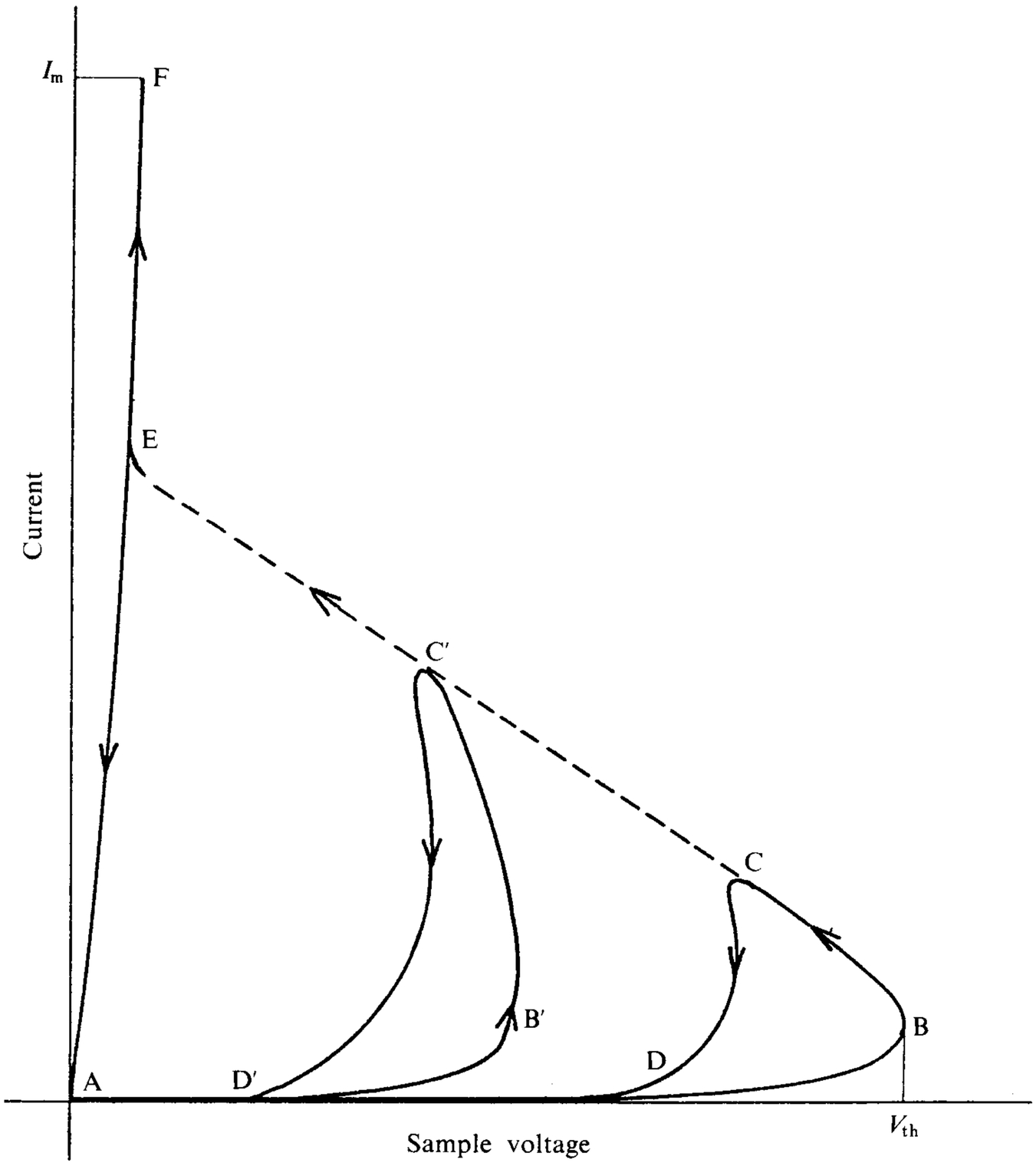

Fig. 1 AC I–V characteristic of the formed sample. Cuve A–B corresponds to the off state. Curve A–E–F to the on-state. Normally, the time sequence of switching is A–B–E–F–A and Switching Occurs from B to E. The reduction of I_m resulted in the hysteresis, curve A–B'–C'–D' which was accompanied by the decreasing in V_{th}.

Fig.2. Threshold voltage V_{th} in every six seconds were recorded. This change of V_{th} seems to have the strong correlation to partial pressure of oxygen in the ambient. For the observation of this change of V_{th}, I_m larger than about 1 mA was needed. The switching was also observed under the current-limited condition. ($I_m < 10\ \mu$A, typical in pure sample and thin film sample) DC I–V characteristic showed switching as in Fig. 3. This characteristic was not affected by the change of partial pressure of oxygen in measurement but changed with the number of switching cycles. At first, lamp voltage was applied to the sample. When the current reached a set value, the voltage was removed instantly. After a few seconds, lamp voltage was applied again[22]. This cycle was repeated automatically, and the sample voltage vs time characteristic was recorded by X–Y recorder. The maximum voltage which was recorded in each cycle corresponded to V_{th}. At the same time, the appearance of I–V characteristic was checked with an oscilloscope on every cycle. As the switching was repeated, V_{th} decreased and the conduction changed from ohmic to non-ohmic in the region near V_{th} as shown in Fig. 3. The threshold voltage V_{th} decreased with increasing number of the continuous cyckes of switching and increased with the pause of switching cycles as shown in Fig. 4. But V_{th} remained constant in every cycle of switching at low temperature as in LN and switching itself was very stable.

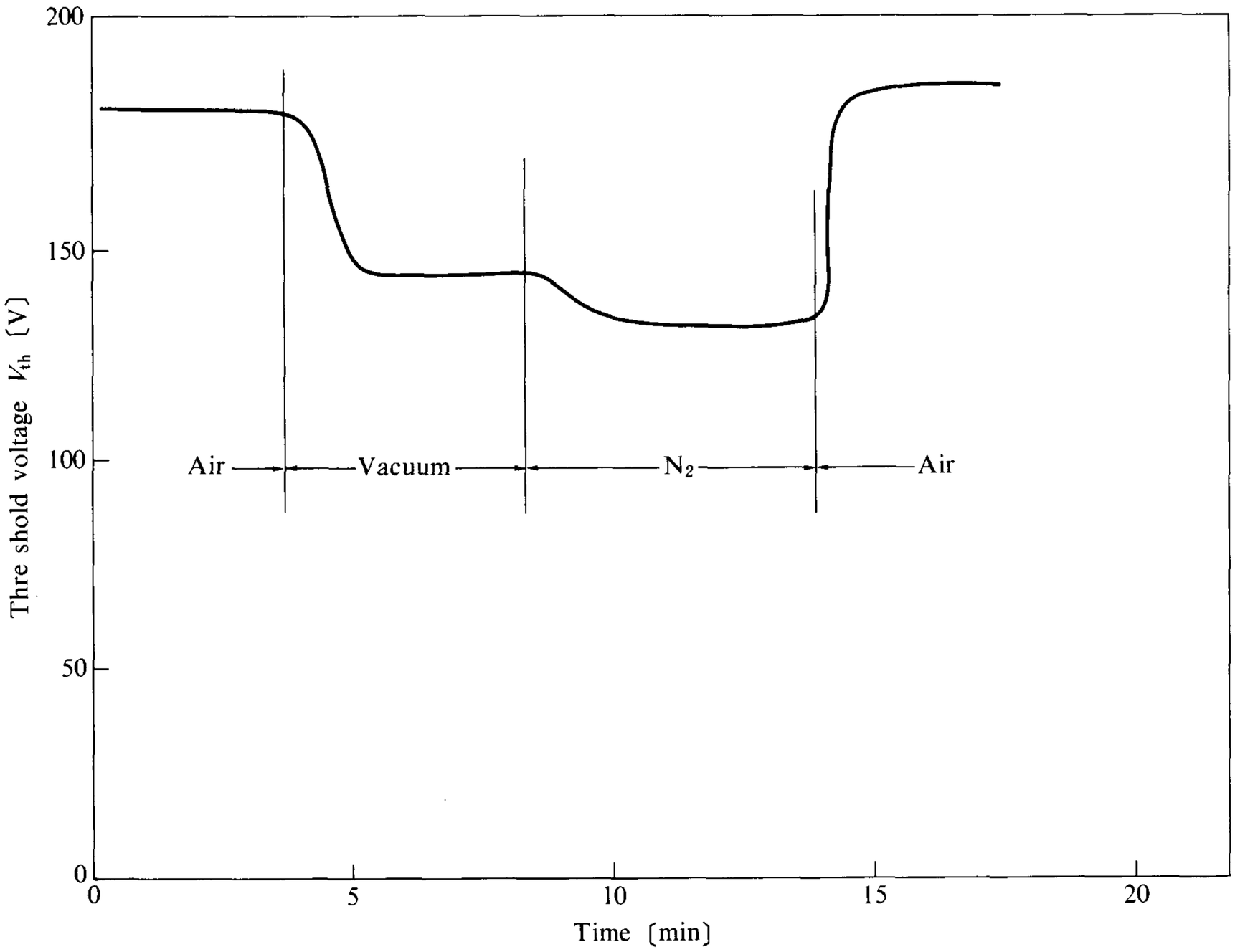

Fig. 2 Typical change of V_{th} of mixed sample with the change of ambient gas condition. Change of V_{th} in cyclic switching in every six seconds were recorded. Maximum current I_m was 3 mA.

3.3 Static DC I–V characteristic

Static DC I–V characteristics were measured by PA DC voltage source. Typical I–V characteristic is shown in Fig. 5. In low electric fields, ohm's law was obeyed i.e., $1 \propto V$, then the steepness region in the curve was followed by the curve in which power law was obeyed i.e., $1 \propto V^2$ or $1 \propto V^3$. Under the current limited condition ($I_m < 10\,\mu$A), no hysteresis was observed in the I–V characteristic. This I–V characteristic sustained the powe relationship (as mentioned above) between 77 and 500 K. In low electric field, the currents were small and the curve steeper at low temperature. Similar I–V relationships have been reported in polycrystalline TiO_2 thin films and CdS single crystals[25,26].

3.4 Pulse measurements

Ordinarilly V_{th} remained constant at low temperature, so, the pulse measurement was done at 77 k. Switching delay time was detected by the application of voltage pulse. Switching delay time depended on the applied voltage as shown in Fig. 6. Overall delay time of the double pulse test is also presented in Fig. 7. Double pulse test consists of the application a positive voltage pulse, whose amplitude is greater than the threshold voltage for switching, followed immediatery by an equal amplitude negative pulse applied before switching occurs. Overall delay time corresponds to the time required for the occurrence of switching from the application of the first positive pulse. When the same amplitude of voltage was applied, overall delay time was longer than that for single pulse alone. The responses of the sample current for the voltage pulse are shown in Fig. 8.

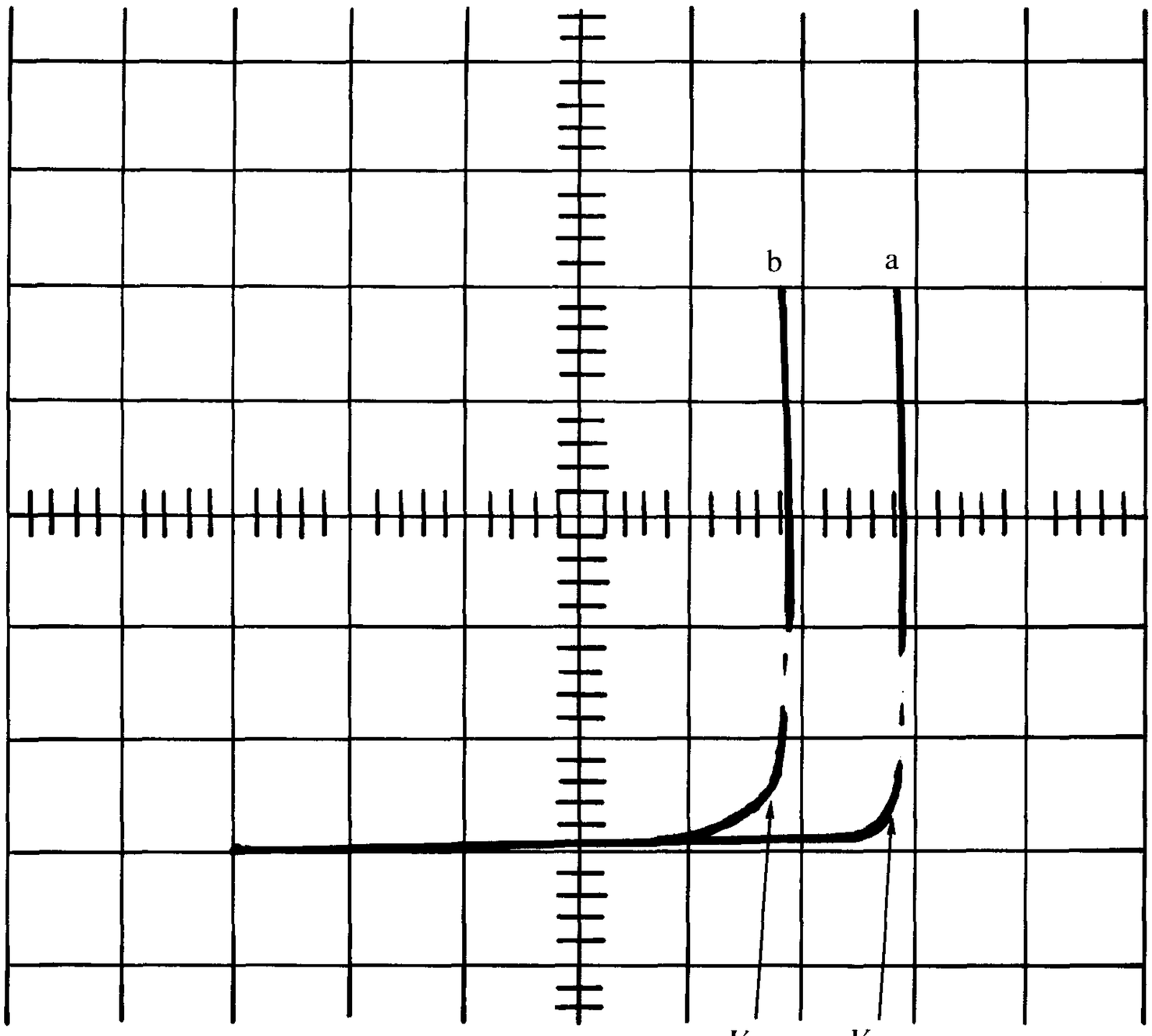

a : The first cycle
b : The second cycle

Fig. 3 DC I–V characteristics of a sample under the current limited condition. I_m was limited to 5 μA. DC lamp voltage was applied to the sample and switching was observed at V_{th}. Vertical scale: 1 μA/div. horizontal scale: 1 v/div.

4. Discussions

Conductance switching was obtained in sintered ferric oxide after the formation of the conductive path by the dessociation of hematite to magnetite. Ferric oxide dessosiates into magnetite at 1392°C in air. The possibility of the appearance FeO or metal Fe can be discarded from the phase diagram of the system Fe–O. High conductive ohmic on-state was obtainable in the forming process. This on-state memory showed breaks at 120 k in the curve of log. R vs $1/T$ characteristic as same as the Verwey transition in magnetite[22]. These facts indicate that the on-state memory is a result of the formation of a magnetite filament. The formed filament must be covered with the reoxidized hematite layer. X-ray back Laue method indicated the phase of hematite on he surface of the conductive path.

The appearance of the reoxidized layer (hematite) causes the resistance increase and makes the ohmic characteristic change into non-ohmic and finally results in the appearance of the off-state. Thus, the change between memory states (ohmic on-state and others) are mostly affected by thermally induced chemical reaction in the conductive path. The resistance of the ohmic on-state memory began to increase at about 600 K in air. This increase of resistance was suppressed in N_2 gas or in vacuum. Similar increase was obtained at room temperature in air by flowing current in the path. This increase of resistance was the

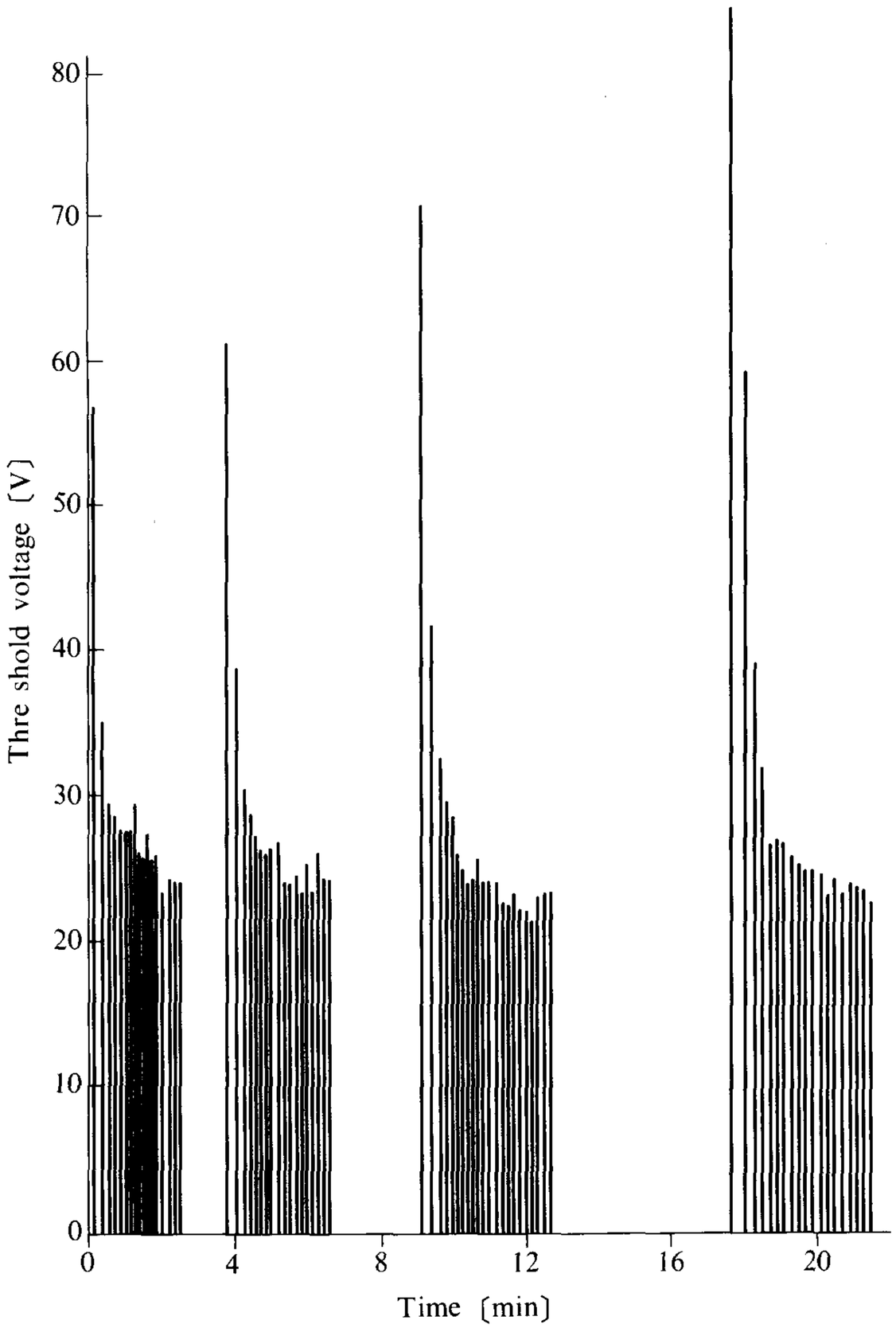

Fig. 4 Threshold voltage V_{th} in the switching cycles. Change of V_{th} as a factor of the continious cycles of switching and as the length of the pause time.

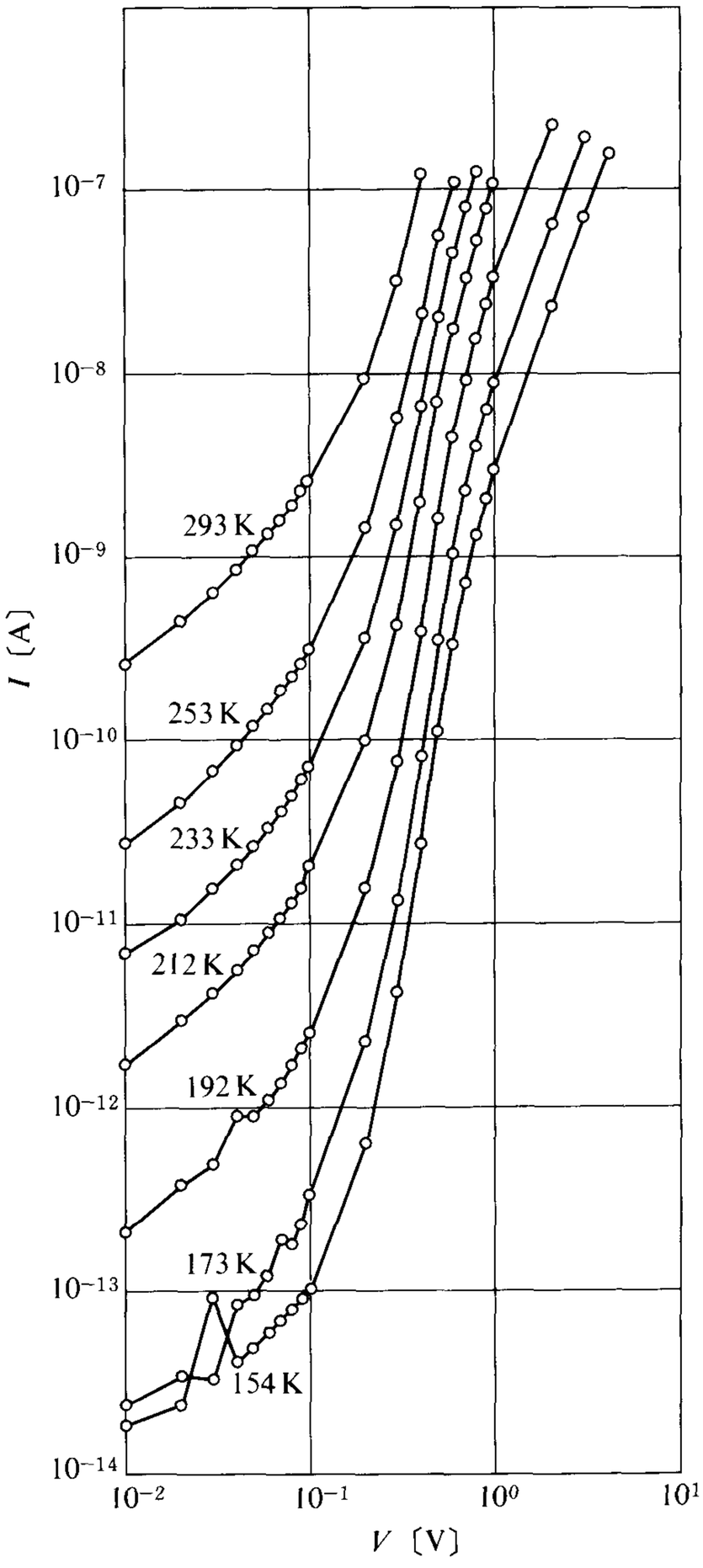

Fig. 5 Static DC I–V characteristics. In the low voltage region ohmic resistance increased the value with temperature. Lampert's triangle was observed.

result of the surface oxidation of magnetite as reported by Bevan et al.[29] The conduction path of the switching sample is same as that of magnetite-hematite-magnetite sandwitch structure.

AC I–V characteristic in Fig. 1 showing negative resistance and memory switching contains the effect of the load resistance in the measuring circuit. Joule heating by the flowing current after switching resulted in the change of the characteristic of memory state. The mechanism of this change consists of the structural change of the surface in magnetite-hematite-magnetite sandwitch structure. So. the resistance of the off-state was affected by number of cycle switching and by the atomospheric partial pressure of oxygen. Then V_{th} of each switching was also affected by the partial pressure of oxygen as in Fig. 2. However, under the condition of small current, V_{th} was not affected by the partial pressure of oxygen. So, the change of V_{th} in the case presented in Fig. 3 and Fig. 4 is not a result of the structural change (oxidation or reoxidation) of the sandwitch structure. From these facts mentioned

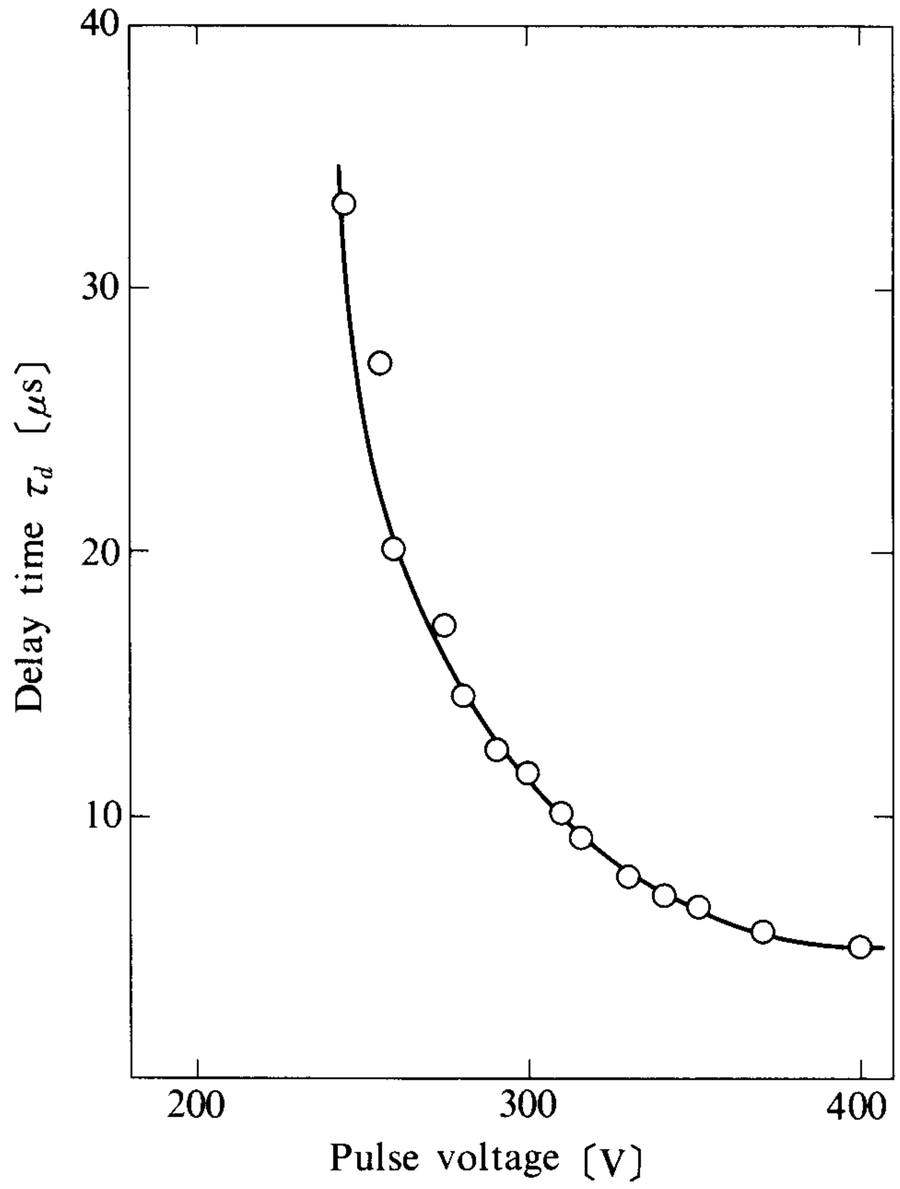

Fig. 6 Switching delay time under the single pulse application at 77 k.

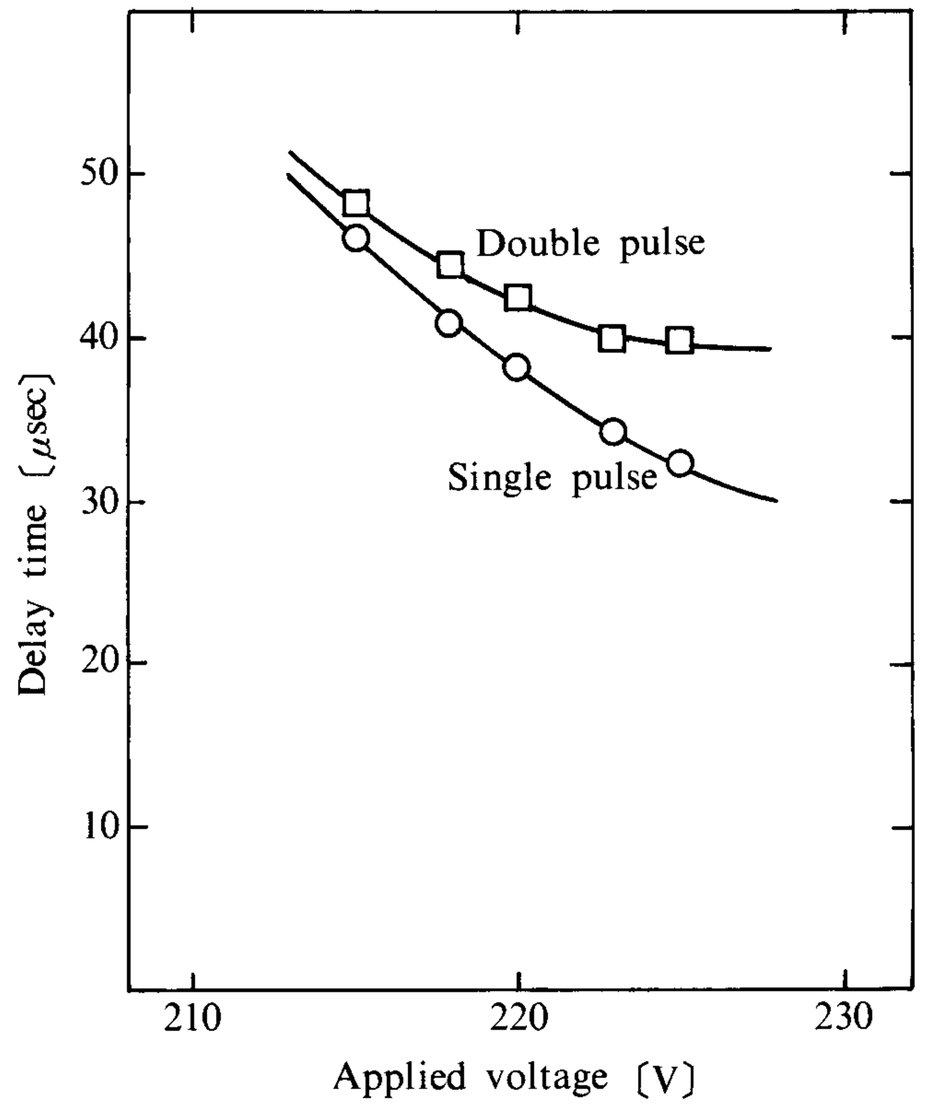

Fig. 7 Switching delay time vs applied pulse voltage (single pulse). Over-all delay time vs applied pulse voltage (double pulse). Both data were obtained at 77 k. Pulse width: 60 μsec.

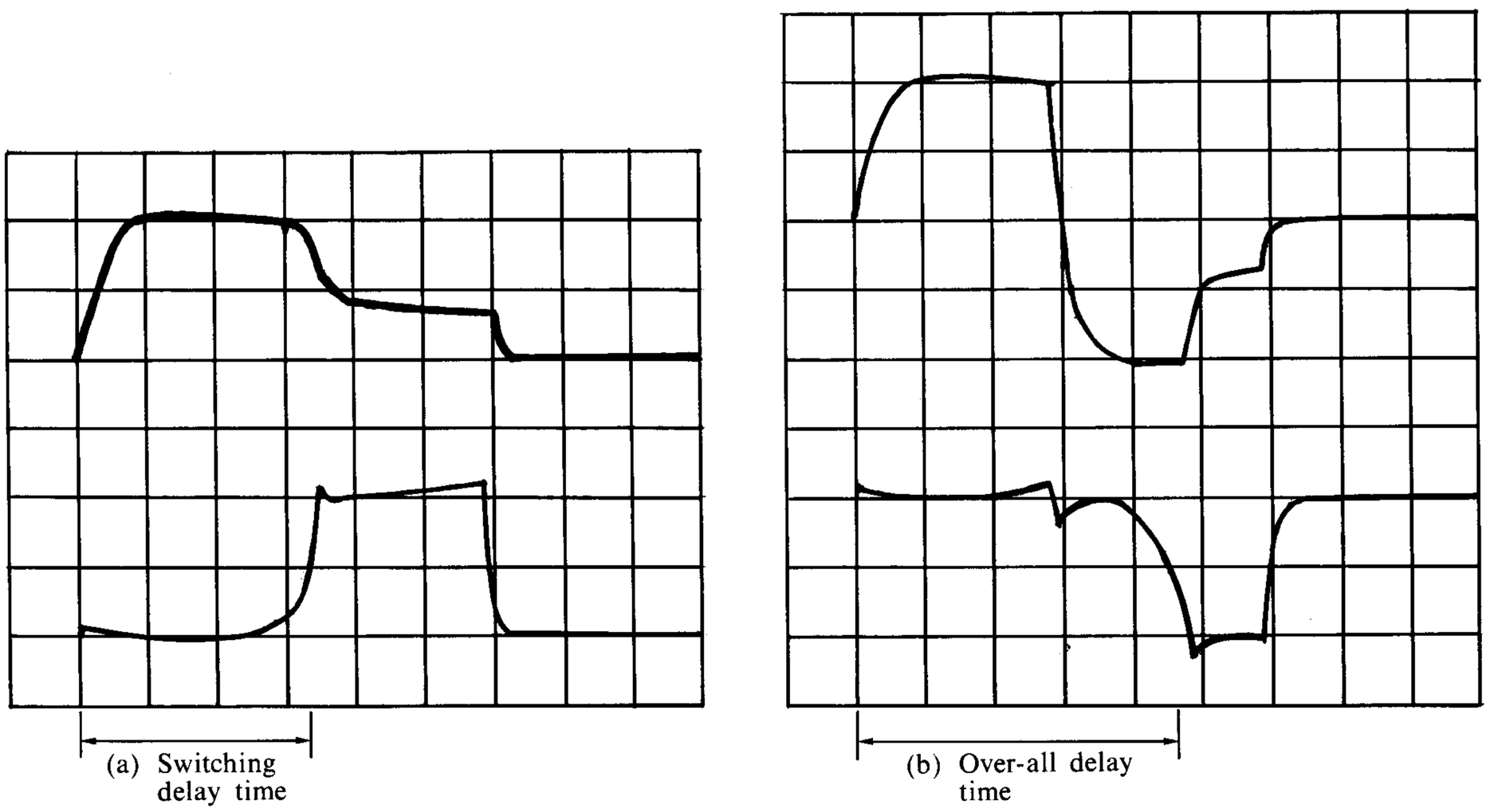

Fig. 8 The responce of the sample current for the voltage pulse.
a) Single pulse application. Upper trace: sample voltage, 100 V/div; lower trace: sample current, 5 mA/div.; time 10 μsec/div.
b) Double pulse application.
a), b) at 77 K

above, Joule heating can be ruled out from the primary cause of switching in ferric oxide.

Static DC I–V characteristic presented in Fig. 5 is indicative of the space charge limited current. Lampert's tirangle[30] is seen in the I–V characteristic. At low electric fields charge carriers are thermally equilibrated (ohmic region) and at high electric fields injected carriers exceed the number of thermally equilibrated ones at a critical voltage V_{tr}. (Eq. 2) And then, I–V characteristic begins to show the relationship $I \propto V^2$. This relationship may be covered by the presence of traps and when traps are all filled with charge carriers, the relationship $I \propto V^2$ will appear in the I–V characteristic. Trap-filled-limit voltage V_{TFL} at which the transition from ohm's law to SCL current flow takes place is given by

$$V_{TFL} = \frac{eN_t L^2}{\varepsilon} \qquad (1)^{30}$$

and

$$V_{tr} = \frac{enL^2}{\varepsilon} \qquad (2)^{30}$$

where L, e, ε, n and N_t are spacing between electrodes, electron charge, static dielectric constant, density of free carriers and density of trap, respectively. In the case of this study, L corresponds to the thickness of hematite layer in magnetite-hematite-magnetite sandwitch structure and remaines constant. In the case of thin film samples the value of L corresponds to the thicness of hematite, and can be estimated actualy. Then, from the curves in Fig. 5, n, N_t and μ_n were culculated using equations (1), (2) and Child's equation. Results are given in table 1. Temperature dependence of μ_n and $1/R$ (R: ohmic resistanse in the curves of Fig. 5 in low voltage region) are shown in Fig. 9. Activation energies for μ_n and $1/R$ from curves in Fig. 9 are 0.23 and 0.29[eV] respectively. On the other hand, n seems to have a weak correlation with temperatures. So, the temperature dependence of ohmic resistance is due mainly to the change in electron mobility. The value of ε is assumed to be constant in the experiment of continuous cycles of switching when the increasing late of applied lamp voltage and ambient temperature are constant. Injected carriers may fill traps at V_{th} and switching occurs. After the removal of applied lamp voltage, effective density of traps increases with time. This means that charge carriers are released from filled traps according to some types of relaxation process. If there are different types of traps and paticular-type traps among others have large capture rate of charge carriers, effective density of traps N_{teff} corresponds to the density of the paticular type. Fig. 10 shows the equivaelent circuit for the relaxation process.

$$N_{teff} = N_t \left\{ 1 - \exp\left(-\frac{t}{\tau} \right) \right\} \qquad (3)$$

Table 1 Culculated value of n, N_t and μ_n from curves shown in Fig. 5. Film thickness: $L = 880$[nm]

T[°C]	n[cm^{-3}]	N_t[cm^{-3}]	μ_n[cm^2/V·sec]	R[Ω]
20	1.77×10^{13}	1.57×10^{14}	8.73×10^{-5}	3.75×10^{7}
−20	5.43×10^{13}	2.74×10^{14}	7.89×10^{-7}	4.00×10^{8}
−40	3.09×10^{13}	3.66×10^{14}	2.55×10^{-7}	1.70×10^{9}
−60	2.17×10^{13}	4.57×10^{14}	1.23×10^{-7}	5.70×10^{9}
−80	1.26×10^{13}	4.23×10^{14}	2.62×10^{-8}	4.00×10^{10}
−100	0.83×10^{13}	6.00×10^{14}	4.37×10^{-9}	3.90×10^{11}
−120	1.09×10^{13}	5.03×10^{14}	1.67×10^{-9}	1.00×10^{12}

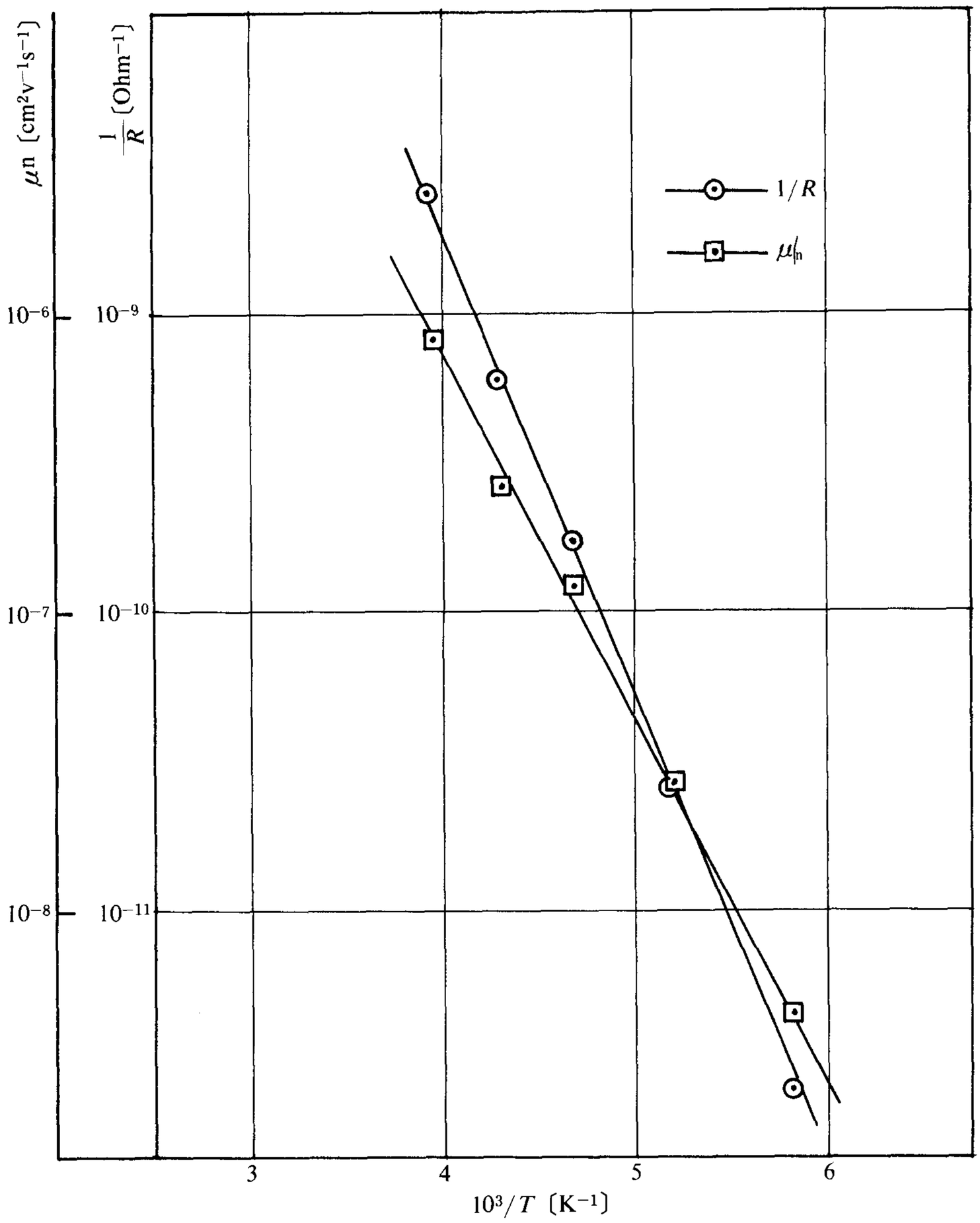

Fig. 9 Temperature dependence of log 1/R and log μ_n R: Ohmic resistance obtained from curves in the low voltage region μ_n: electron mobility Both R and μ_n are culculated from data shown in Fig. 5

From equations (1) and (3),

$$V_{th}=V_{TFL}=\frac{eL^2N_t}{\varepsilon}\left\{1-\exp\left(-\frac{t}{\tau}\right)\right\} \tag{4}$$

where

$$\tau=\frac{R+r}{\dfrac{1}{C_1}+\dfrac{1}{C_2}} \tag{5}$$

If R+r corresponds to the off state resistance ($\sim 10^9$ ohm), and $C_1=C_2=10^{-9}$[F] then $\tau=0.5$[s]. From equation (4), the change of V_{th} in the experiment of continuous cycles of switching, shown in Fig. 4 can be explainable. In the continuous cycles of switching, charges filled in the paticular-type traps drop into other ones during the time after removal of ap-

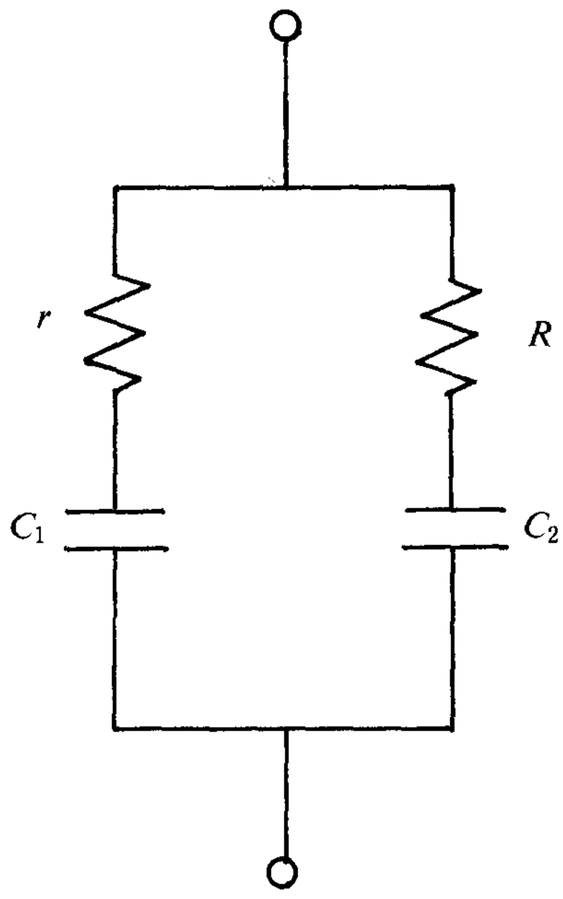

Fig. 10 Equivalent circuit for the explanation of relaxation process such as charge trapping and release. C_1 and C_2 correspond to traps of different type.

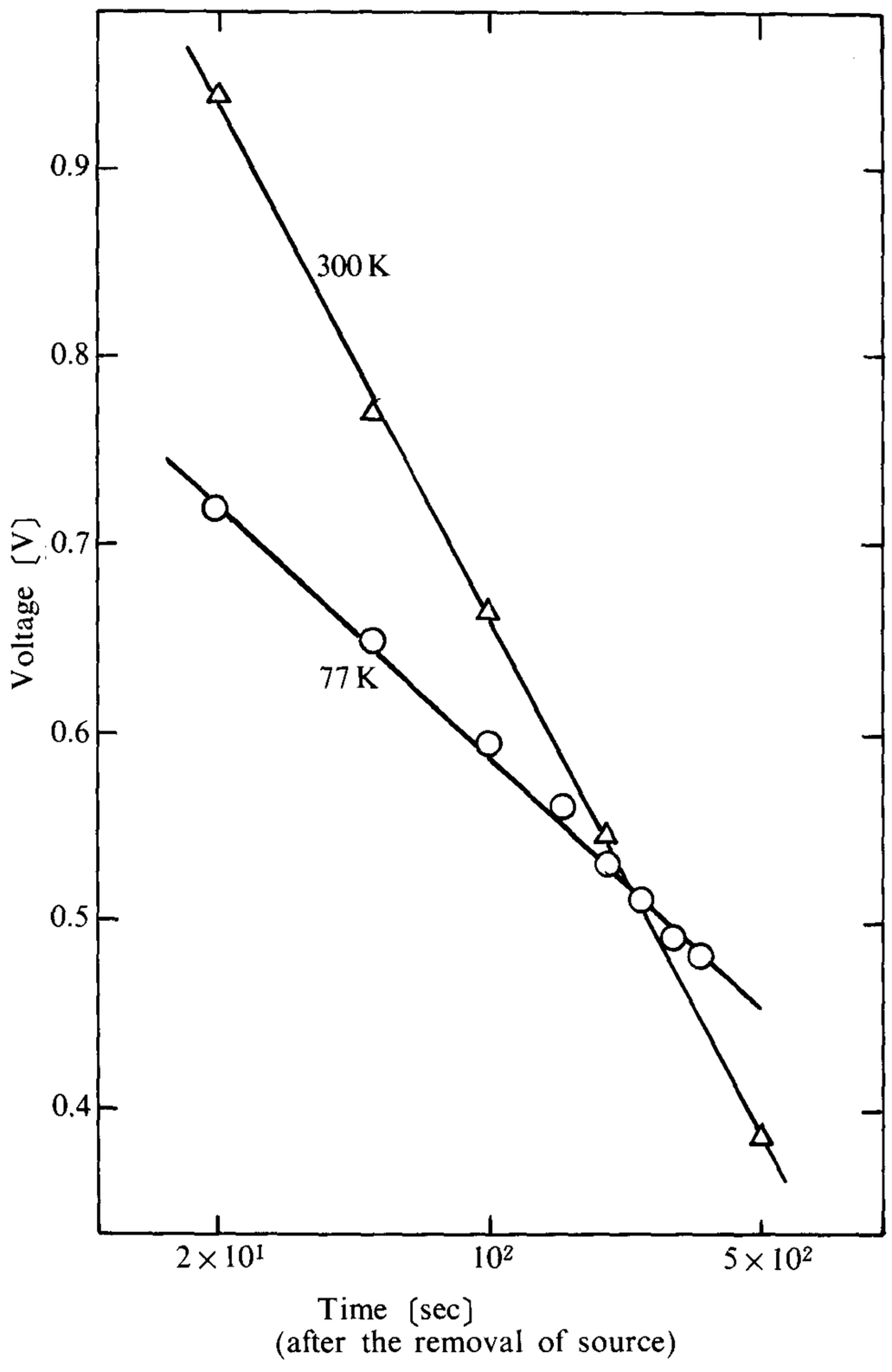

Fig. 11 Potential defference observed between electrodes of switching sample after removal of voltage source.

plied voltage. As charges in the other traps increase, residual charges in the paticular-type traps increase at every switching. Then effective trap density N_{teff} in equation (3) decreases and V_{th} (V_{TFL}) also decreases gradually. The increase of V_{th} with increasing the length of pause time is the consequence of discharging of all traps.

Residual charge in the sample after the removal of source produced the potential difference between the electrodes. And this potential difference decreases as time as shown in Fig. 11. This characteristic may be the result of the exitation of trapped carriers. Pulse measurement denied the possibility of double injection mechanism in hematite switching sample. The fact that overall delay time for double pulse was shorter than delay time for single pulse indicated the possibility of a single carrier injection mechanism. But, no detailed nature of traps and mechanisms of injection has been obtainable only through the present data.

5. Conclusions

Conductance switching in iron oxides was observed both in sintered samples and thin films. In sintered samples, switching occurs after the formation of the conductive path composing a sandwitch structure of magnetite-hematite-magnetite. At high electric fields single carrier injection occured and space-charge-limited current flows through high resistive Fe_2O_3 (hematite) layer which has some types of traps. Trapped charges caused the potential defference between the electrodes. No structural change occured in the sandwitch structure when the flowing current was small and Joule heating was negligible. In this case the characteristic of stable switching had no dependence on the change of surrounding gas atmosphere. Threshold voltage V_{th} corresponded to trap-filled-limit voltage V_{TFL} in Lampert's triangle. The change of effective density of traps caused by trapping or release of charge carriers gave the systematic change of V_{th}. However, if large current flow after switching, Joule heating caused the structural change in the sandwitch structure and V_{th} of each switching was affected by the change by the change of sorrouning gas atmosphere.

Acknowledgement

The auther wish to thank Mr. H. Takahashi for his cooperation throughout this study and Mr. N. Nakamura for his help with the experiments.
(Received, Sept. 30, 1984)

References

1) D. V. Geppert, Proc. IEEE 223 (1963)
2) T. W. Hickmott and W. R. Hiatt, Sol. St. Elec. 13, 1033 (1970)
3) J. F. Gibbons and W. E. Beadle, Sol. St. Elec. 7, 785 (1964)
4) B. Lalevic, N. Fushillo and B. Leung, Phys. Stat. Sol. 23, 61 (1974)
5) Shih-Fang Lo, Proc. IEEE 609 (1964)
6) C. Pettus, Proc. IEEE 98 (1965)
7) K. L. Chopra, J. Appl. Phys. 36, 184 (1965)
8) F. Argall, Sol. St. Elec. 11, 535 (1968)
9) Earl L. Cook, J. Appl. Phys. 41, 551 (1970)
10) M. J. Zarabi and M. Satyam, J. Appl. Phys. 45, 775 (1974)
11) D. C. Bullock and D. J. Epstein, Appl. Phys. Lett. 17, 199 (1970)
12) C. W. Wilmsen and M. C. Allender, J. Appl. Phys. 45, 1912 (1974)
13) T. Takahashi and O. Yamada, J. Appl. Phys. 48, 1258 (1977)
14) Y. Taketa and R. Furugochi, Appl. Phys. Lett. 31, 405 (1977)

15) H. Fritzche, IBM J. Res. Dev. 13, 515 (1969)
16) K. E. Petersen and D. Adler, Appl. Phys. Lett. 25, 211 (1974)
17) K. van Steensel, F. van de Burg and C. Kooy, Phyl. Res. Repts. 22, 170 (1967)
18) R. C. Morris, J. E. Christopher and R. V. Coleman, Phys. Rev. 184, 565 (1969)
19) A. D. Pearson and C. E. Miller, Appl. Phys. Lett. 14, 280 (1969)
20) M. Miyamoto, T. Suzuki, M. Kindaichi and Y. Mita, Jap. J. Soc. Powder. P. Metall. 21, 205 (1974)
21) M. Miyamoto, T. Suzuki, M. Kindaichi, J. Shinohara and Y. Mita Jap. J. Soc Powder P. Metall. 23, 235 (1976)
22) M. Miyamoto, Trans. Kokushikan Univ. Facul. Eng. 11, 52 (1978)
23) G. Tailor and B. Lalevic, J. Appl. Phys. 48, 4410 (1977)
24) M. Miyamoto, Trans. Kokushikan Univ. Facul. Eng. 17, 75 (1984)
25) C. W. Litton and D. C. Reynolds, Phys. Rev. 133, 536 (1964)
26) R. W. Smith and A. Rose, Phys. Rev. 97, (6) 1531 (1955)
27) L. S. Darken and R. W. Gurry, J. Amer. Chem. Soc. 68, 798 (1946)
28) D. J. M. Bevan, J. P. Shelton and J. S. Anderson, J. Chem. Soc. 1729 (1948)
29) U. Colombo, G. Fagherazzi, F. Gazzarrini, G. Lanzavecchia and G. Sironi, Nature 202, 175 (1964)
30) Murray A. Lamepert, Phys. Rev. 103, (6) 1648 (1956)